

Induction of G₂/M Phase Arrest and Apoptosis by Oridonin in Human Laryngeal Carcinoma Cells

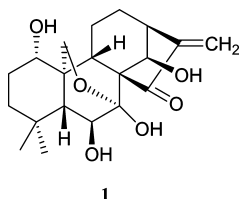
Ning Kang,^{†,‡} Jing-Hai Zhang,[‡] Feng Qiu,[§] Sheng Chen,[‡] Shin-ichi Tashiro,[⊥] Satoshi Onodera,[⊥] and Takashi Ikejima^{*‡}

China-Japan Research Institute of Medical and Pharmaceutical Sciences, Shenyang Pharmaceutical University, 103 Wenhua Road, Shenyang, 110016, People's Republic of China, Department of Biochemistry and Molecular Biology, Shenyang Pharmaceutical University, 103 Wenhua Road, Shenyang, 110016, People's Republic of China, Department of Natural Products Chemistry, Shenyang Pharmaceutical University, 103 Wenhua Road, Shenyang, 110016, People's Republic of China, and Department of Clinical and Biomedical Science, Showa Pharmaceutical University, Tokyo 194-8543, Japan

Received December 16, 2009

Oridonin (**1**), an active component isolated from the plant *Rabdosia rubescens*, has been reported to exhibit antitumor effects. In this study, the mechanism involved in **1**-induced growth inhibition, including apoptosis and G₂/M phase arrest, in human laryngeal carcinoma HEP-2 cells deficient in functional p53, was investigated for the first time. Compound **1** triggered the mitochondrial apoptotic pathway, as indicated by increased Bax/Bcl-2 ratios, reduction of mitochondrial membrane potential ($\Delta\Psi_m$), and substantial increase in apoptosis-inducing factor (AIF) and cytochrome *c*. Inhibition of caspase-9 in HEP-2 cells did not protect the cells from **1**-induced apoptosis, and cleaved caspase-9 was not detected, indicating that apoptosis occurred via a caspase-9-independent pathway. The results also suggested that G₂/M phase arrest and apoptosis mediated by **1** occurred via a p53-independent but in a p21/WAF1-dependent manner in HEP-2 cells. In addition, the generation of reactive oxygen species (ROS) was found to be a critical mediator in growth inhibition induced by **1**. Taken together, the results indicate that oridonin (**1**) is a potentially effective agent for the treatment of laryngeal squamous cell carcinoma.

A significant proportion of anticancer drugs are directly or indirectly derived from medicinal plants, which still continue to provide essential sources of novel discovery leads.¹ Oridonin (**1**), an active diterpenoid isolated from the plant *Rabdosia rubescens* (Hemsl.) Hara (Lamiaceae), has been used for the treatment of various human diseases due to its anti-inflammatory, antibacterial, and antitumor effects.^{2,3} Its *ent*-kaurene structure is thought to be the active domain for anticancer activity.^{4,5} Previous reports have demonstrated that **1** exhibits marked inhibitory effects in vivo on prostate carcinoma, non-small-cell lung cancers, acute myeloid leukemia, and glioblastoma multiforme and has in vitro activity against melanoma, fibrosarcoma, breast, and cervix tumor-derived cell lines.^{6–8} However, little is known about the mechanisms underlying the effects of **1** on human laryngeal cancer cells.



Laryngeal squamous cell carcinoma (LSCC) is the most common squamous cell carcinoma of the head and neck, and there is a steady annual increase in new cases and deaths.⁹ Epidemiological studies have revealed that the incidence rates vary from country to country and in different population groups.¹⁰ LSCC accounts for 1–8.4% of total human cancers in mainland China.¹¹ The curative effect and prognosis of the required operation are relatively poor and are generally followed by severe dysfunction and recrudescence. During

recent decades, combined modality approaches have been developed, and chemotherapy has been confirmed as a major component of these treatment approaches to improve survival in patients with advanced laryngeal cancer.^{12,13} However, the overall survival for patients with advanced LSCC has not been improved significantly.

The p53 protein is the “guardian of genome integrity”, since it elicits a block in the cell cycle, DNA repair, and, eventually, an apoptotic response after stress insults, compromising genomic integrity, oncogene activation, and hypoxia.¹⁴ Mutations in the *p53* gene are involved in acquired and intrinsic treatment resistance in human tumors and render tumor cells refractory to many anticancer therapies.^{15,16} Nonfunctional or mutated p53 protein has been found in LSCC.^{17,18} This is one of the main reasons to search for new anticancer compounds that are more effective in unresponsive tumors, with reduced adverse effects and with original mechanisms of action, to improve the general outcome of cancer chemotherapy. Many compounds that have some use in p53-defective cancer chemotherapy, e.g., mistletoe lectin and berberine, are derived from plant sources.^{19,20} Therefore, our group has begun to screen for valid compounds derived from plant sources that might be applied to LSCC treatment.

The present study was designed to examine the efficacy and associated mechanism of action of oridonin (**1**) in HEP-2 cells lacking functional p53 protein.^{21,22} Evidence is provided that **1** significantly induced G₂/M arrest and apoptosis via ROS generation in HEP-2 cells. To further establish the anticancer mechanism of **1**, the levels of cell cycle control- and apoptosis-related molecules, which are strongly associated with the programmed cell death signal transduction pathway and affect the chemosensitivity of tumor cells to anticancer agents, were assayed. During the course of characterizing the role of the mitochondrial pathway in the apoptosis of HEP-2 cells, an unexpected observation was made that inhibition of caspase-9 can enhance (rather than retard) apoptosis to selected stimuli.

Results and Discussion

Cytotoxic Effect of Oridonin (1) against HEP-2 Cells. To detect the cytotoxic effects of **1** on HEP-2 cells, the cells were

* To whom correspondence should be addressed. Tel: +86-24-2384-4463. Fax: +86-24-2384-4463. E-mail: ikejimat@vip.sina.com.

[†] China-Japan Research Institute of Medical and Pharmaceutical Sciences, Shenyang Pharmaceutical University.

[‡] Department of Biochemistry and Molecular Biology, Shenyang Pharmaceutical University.

[§] Department of Natural Products Chemistry, Shenyang Pharmaceutical University.

[⊥] Showa Pharmaceutical University.

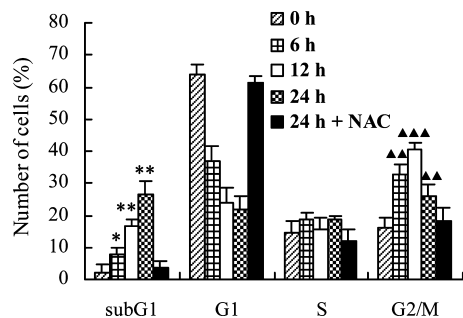


Figure 1. Apoptosis and G₂/M arrest were induced by oridonin (**1**) and were inhibited by NAC treatment in HEP-2 cells. The cells were cultured in the presence of 36 μ M oridonin for 0, 6, 12, and 24 h or co-incubated with 2.5 mM NAC for 24 h. Then, the cells were stained with PI at 37 °C for 30 min and measured by flow cytometry after collection. The percentage of cells in different phases of the cell cycle was represented by a bar diagram. The values shown are means \pm standard error ($n = 3$) (* $p < 0.05$, ** $p < 0.01$ vs the subG1 phase percentage in groups not treated with **1**; $\blacktriangle\blacktriangle p < 0.01$, $\blacktriangle\blacktriangle\blacktriangle p < 0.001$ vs the G₂/M phase percentage in groups not treated with **1**).

cultured with 10.7–81 μ M compound **1** for 6, 12, 24, 36, and 48 h. Oridonin induced cell death in a dose- and time-dependent manner. The IC₅₀ for 24 h compound **1** treatment was 37.1 μ M. Treatment of HEP-2 cells with 36 μ M **1** for 24 h resulted in approximately 50% cell death (Figure S1, Supporting Information).

Oridonin (1)-Induced Apoptotic Cell Death in HEP-2 Cells. To determine the features of **1**-induced HEP-2 cell growth inhibition, flow cytometric analysis was carried out. Incubation of fixed and permeabilized cells with propidium iodide (PI) resulted in quantitative PI binding with total cellular DNA, and the fluorescence intensity of PI-labeled cells was proportional to the DNA content. Apoptotic nuclei with hypodiploid DNA content corresponded to the subG1 peak. As shown in Figure 1, oridonin induced a significant time-dependent increase in the proportion of subG1 cells. In the control group, the percentage of subG1 cells was about 2.3%. A maximal increase in the frequency of subG1 cells was observed after 24 h of treatment with 36 μ M **1** (26.57%).

To confirm whether treatment with **1** resulted in apoptotic cell death, the morphologic changes of the cells were examined by phase-contrast microscopy, fluorescence microscopy, and transmission electron microscopy. Compared with the control group, significant morphologic changes, such as membrane blebbing, chromatin condensation and margination at the nuclear periphery, and the presence of granular apoptotic bodies, were observed in the cells treated with 36 μ M **1** for 24 h (Figure S2, Supporting Information). These results suggested that **1** can induce apoptotic cell death in HEP-2 cells.

Oridonin (1) Caused G₂/M Cell Cycle Arrest in HEP-2 Cells. As shown in Figure 1, exposure of HEP-2 cells to compound **1** resulted in the increased accumulation of cells in the G₂/M phase. The percentages of the G₂/M phase were increased from 16.32% in untreated cells to 32.84%, 40.57%, and 25.84% in cells treated with **1** for 6, 12, and 24 h, respectively. In this experiment, maximum accumulation of cells in the G₂/M phase was observed after treatment of cells with 36 μ M **1** for 12 h, which was reduced after an exposure of 24 h. Interestingly, the decrease in the percentage of cells in the G₂/M phase after 24 h of treatment with **1** was associated with a concomitant increase in apoptosis (Figure 1). It is well known that cells have evolved a series of checkpoints, which prevent them from entering a new phase until they have successfully completed the previous one, to ensure proper progression through the cell cycle. These checkpoints allow progression through the cell cycle or arrest the cells in the G₂/M phase in response to DNA damage for DNA repair.^{23,24} Cell cycle arrest

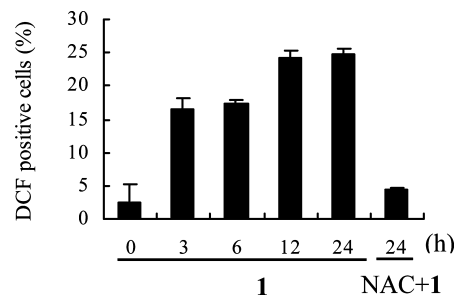


Figure 2. Persistent ROS generation was induced by oridonin (**1**) and blocked by NAC in HEP-2 cells. The cells were cultured in the presence of 36 μ M **1** for 0, 3, 6, 12, and 24 h or co-incubated with 2.5 mM NAC for 24 h. DCF, the fluorescent dye product of peroxidized DCF-DA, was measured fluorometrically at 1 h post-treatment. Values are expressed as the mean \pm standard errors ($n = 3$).

may lead to apoptotic cell death in the case of severe DNA damage. The present results suggest that the DNA damage in HEP-2 cells caused by **1** at 24 h may be irreparable, and this, therefore, forces the arrested cells into apoptosis.

Oridonin (1) Triggered ROS Early Generation That Mediated HEP-2 Apoptosis and Cell Cycle Arrest. To investigate whether **1** stimulated ROS generation in HEP-2 cells, the intracellular ROS levels were measured using the ROS-detecting fluorescent dye 2',7'-dichlorofluorescein diacetate (DCF-DA). After HEP-2 cells were exposed to 36 μ M **1** for the indicated time periods, moderate generation of ROS was observed at 3 h (approximately 7-fold), and the level of ROS increased slowly over 24 h. The ratio of DCF-positive cells was 2.56%, 16.65%, 17.25%, 24.21%, and 24.86% at 0, 3, 6, 12, and 24 h, respectively. As expected, a well-known ROS scavenger, *N*-acetylcysteine (NAC), at 2.5 mM, markedly decreased the level of ROS from 24.86% to 4.41% at 24 h (Figure 2; Figure S3, Supporting Information). On the other hand, when the cells were pretreated with 2.5 mM NAC for 1 h and then with **1** for the indicated time periods, the levels of apoptosis and cell cycle arrest were significantly lower than those of the cells treated with oridonin alone. As shown in Figure 1, when co-incubated with NAC, the percentage of the subG1 phase was reduced from 26.57% for **1** alone to 3.39% at 24 h, and the same was the case with the G₂/M phase: when co-incubated with NAC, the percentage of the G₂/M phase was reduced from 25.84% for **1** alone to 18.14% at 24 h. In addition, morphological changes were also observed using phase-contrast microscopy and fluorescence microscopy with acridine orange (AO) staining. For the 24 h **1**-treated cells, apoptotic bodies and markedly fragmented DNA in nuclei were observed (Figures S2A-b, S2A-e, Supporting Information). In the NAC-co-incubated group, the cells showed only rare apoptotic bodies and nuclear damage (Figures S2A-c, S2A-f, Supporting Information).

Growing evidence suggests that chemotherapeutic agents may be selectively toxic to cancer cells because they increase oxidative stress that can induce various biological responses, such as DNA repair, cell cycle arrest, and/or apoptosis.^{25,26} In the present study, **1** triggered ROS generation, which was found to be related to the oridonin-induced apoptosis and cell cycle arrest in HEP-2 cells.

ROS Reduced the $\Delta\Psi_m$ and Mediated the Oridonin (1)-Induced HEP-2 Apoptosis through the Mitochondrial Signaling Pathway and a Caspase-9-Independent Apoptotic Mechanism. It has been demonstrated that apoptosis involves a disruption of mitochondrial membrane integrity, which plays a key role in cell death.²⁷ The fluorescent probe rhodamine-123 was used to measure the $\Delta\Psi_m$. The decrease in rhodamine-123 fluorescence intensity reflected the loss of $\Delta\Psi_m$. The fluorescence intensity of **1**-treated cells for the indicated time periods was observed by fluorescence microscopy or analyzed by FACScan. The cells

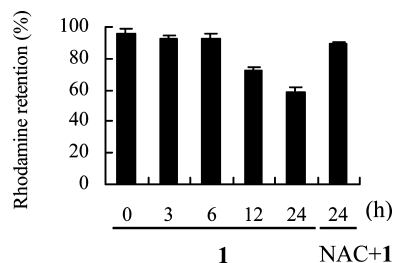


Figure 3. A significant drop in $\Delta\Psi_m$ was induced by oridonin (**1**) and was rescued by NAC in HEp-2 cells. The cells were incubated with $36\ \mu\text{M}$ **1** for 0, 3, 6, 12, and 24 h or a combination of $36\ \mu\text{M}$ **1** with $2.5\ \text{mM}$ NAC for 24 h. Then, the cells were loaded with membrane-sensitive probe rhodamine-123 at $37\ ^\circ\text{C}$ for 30 min, washed, and measured by FACScan flow cytometry after collection. The values shown are mean \pm standard errors ($n = 3$).

incubated with **1** were observed to have a weak green fluorescence compared with the bright green fluorescence of untreated cells (Figures S4A, Supporting Information). Quantitative analysis revealed that minor changes in the $\Delta\Psi_m$ could be observed in the cells treated with **1** alone for 3 and 6 h. When the exposure time was extended to 24 h, a significant change in $\Delta\Psi_m$ was found in the cells treated with **1** alone. Exposure of HEp-2 cells to **1** reduced the fluorescence intensity of rhodamine-123 staining from 95.64% in untreated cells to 58.56% in cells treated for 24 h (Figure 3; Figure S4B, Supporting Information).

To evaluate whether ROS participated in the $\Delta\Psi_m$ regulation, the ROS scavenger NAC was introduced to abolish the effect of ROS. The results obtained showed that combination with NAC markedly reversed the dissipation in $\Delta\Psi_m$, as illustrated by the increased number of rhodamine-positive cells from 58.56% for **1** alone to 89.31% in the presence of NAC at 24 h (Figure 3; Figure S4B, Supporting Information). The same results were also obtained by fluorescence microscopic observations (Figure S4A, Supporting Information). ROS can cause apoptotic cell death via a variety of mechanisms, among which mitochondrial damage plays an important role.²⁸ In the present study, **1**-induced ROS generation appeared to be an early event (about at 3 h), but loss of $\Delta\Psi_m$ was observed more prominently after 6 h of treatment. Addition of NAC to **1**-treated HEp-2 cells effectively blocked the drop in $\Delta\Psi_m$. This finding suggests **1** promoted ROS acting on the mitochondrial membrane potential as another possible mitochondria-directed mechanism in the model used.

It has been shown that the Bcl-2 family plays an essential role in controlling the mitochondrial pathway.^{29,30} This family includes proapoptotic proteins (e.g., Bax, Bad) and antiapoptotic proteins (e.g., Bcl-2, Bcl-xL), and the balance between these two groups determines the fate of cells. Bax can act on the mitochondria to induce the mitochondrial permeability transition, resulting in the release of some components, including cytochrome *c* and AIF.^{31,32} To confirm whether such a mechanism is involved in apoptosis induced by **1**, the expression of Bax, Bcl-2, cytochrome *c*, and AIF was examined by western blot analysis. As shown in Figure 4A, the expression of Bax protein and cytochrome *c* began to increase from 6 and 12 h, respectively, while the Bcl-2 expression markedly decreased at 24 h. Simultaneously, a visible increase in AIF levels was also detectable after only a 6 h incubation. AIF is released from the mitochondria and translocated to the nucleus after an apoptotic signal, where it is capable of inducing nuclear chromatin condensation and large-scale DNA fragmentation to mediate a caspase-independent mitochondrial apoptosis.³³

Cytochrome *c* normally functions via its association with other molecules to form a caspase-9-activating complex, which plays a key role in the caspase-dependent apoptotic pathway.³⁴ Some of our preliminary studies have indicated that **1** is able to inhibit the proliferation of a number of human cancer cell lines via the caspase-

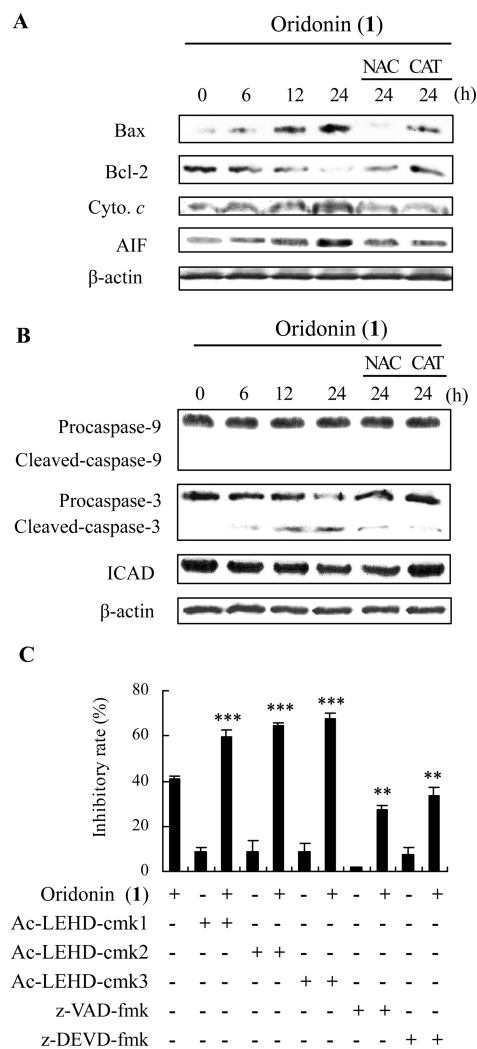


Figure 4. Oridonin (**1**) induced an increased ratio of Bax/Bcl-2, triggering the mitochondrial signaling pathway and mediated a caspase-9-independent apoptosis in HEp-2 cells, and ROS significantly contributed to these apoptotic processes. (A and B) cells were treated with $36\ \mu\text{M}$ **1** in the absence or presence of $2.5\ \text{mM}$ NAC or $500\ \text{U/mL}$ CAT for 0, 6, 12, or 24 h; then cell lysates were separated by 12% SDS-PAGE, and Bax, Bcl-2, cytochrome *c*, and AIF (A) and caspase-9, caspase-3, and ICAD (B) protein expression was detected by western blot analysis. The results shown here are representative of at least three independent experiments. (C) Cells were pretreated with z-VAD-fmk ($10\ \mu\text{M}$), z-DEVD-fmk ($5\ \mu\text{M}$), or Ac-LEHD-cmk (1: $5\ \mu\text{M}$, 2: $10\ \mu\text{M}$, 3: $20\ \mu\text{M}$) for 1 h and then cultured with $36\ \mu\text{M}$ **1** for 24 h. Cell inhibitory ratio was measured by a MTT assay ($n = 3$, mean \pm SD, *** $p < 0.001$, ** $p < 0.01$ vs oridonin alone-treated group).

9-dependent pathway.^{6,35} However, in the present study, **1**-induced apoptosis activation might differ in certain aspects. It is interesting to note that no apparent change was observed in the protein level of pro-caspase-9, and cleaved-caspase-9 could not be detected in **1**-treated HEp-2 cells (Figure 4B). Experiments were therefore conducted to identify which caspases might be involved in the apoptosis process induced by **1**. As shown in Figure 4B, the cleavage process of pro-caspase-3 occurred sequentially in HEp-2 cells exposed to **1** in a time-dependent manner, which was further supported by the degradation of an inhibitor of caspase-activated DNase (ICAD). ICAD is a substrate of caspase 3. When caspase-3 is activated by apoptotic stimuli, ICAD is cleaved, resulting in the release of caspase-activated DNase (CAD), which appears to cause DNA fragmentation in nuclei.³⁶ Numerous studies have shown that caspase-9 is an initiator caspase in many but not all intrinsic

pathways of proapoptotic signaling.^{37,38} Therefore, a functional role for caspase-9 in **1**-induced apoptosis was also suggested by experiments in which irreversible inhibitors of caspase-9, caspase-3, and the pan-caspase inhibitor were introduced. Unexpectedly, the caspase-9 inhibitor (Ac-LEHD-cmk) was found to enhance (rather than retard) apoptosis from stimulus with **1**. The effect of the caspase-9 inhibitor was dose-dependent and observed at concentrations as low as 5 μ M, while the pan-caspase inhibitor, z-VAD-fmk, and the caspase-3 inhibitor, z-DEVD-fmk, could inhibit apoptosis (Figure 4C). Taken collectively, the current findings can be interpreted as follows: **1** triggers a compensatory pathway involving another caspase, such as caspase-3, and at least some types of apoptotic pathways in HEP-2 do not require caspase-9 participation. Recently, Zheng et al. reported that mice deficient in caspase-9 undergo a rapid activation of alternative caspases (notably caspase-2) following Fas cross-linking in vivo.³⁹ Therefore, caspase-8 or caspase-2 might also be involved in **1**-induced caspase-9-independent apoptosis pathways in HEP-2 cells. Further studies are needed to clarify this.

In order to confirm that the mitochondrial signaling pathway was initiated by ROS, the cells were pretreated with NAC and catalase (CAT, hydrogen peroxide decomposer) and then incubated with **1** for 24 h. As shown in Figure 4, NAC and CAT pretreatment significantly reversed the changes in Bax, Bcl-2, AIF, cleaved-caspase-3, and ICAD expressions compared with treatment with **1** alone. The cumulative events demonstrated that ROS accumulation was responsible for modifying the level of antiapoptotic and proapoptotic proteins, thereby causing disruption of $\Delta\Psi_m$ and a substantial increase in AIF, which resulted in the **1**-induced HEP-2 apoptosis.

Expression of Cell Cycle Regulators in Oridonin (1)-Treated HEP-2 Cells. It is now established that the tumor suppressor p53 inhibits cell growth through activation of cell cycle arrest and apoptosis. Lee et al. have reported that p53 arrests the cell cycle in G₂/M by increasing p21/WAF1 levels,⁴⁰ which challenges the present observations because HEP-2 cells are deficient in functional p53.^{21,22} We observed that, despite its mutated p53 status, HEP-2 cells are arrested and delayed in G₂/M progression in response to **1**. The results showed that treatment with **1** of the cells resulted in a time-dependent decrease in the protein expression of cyclin B1 as well as cdc2 (a cyclin-dependent kinase, CDK) in HEP-2 cells (Figure 5A). However, exposure of the cells to **1** resulted in an increase in levels of inactive phospho-cdc2 (Tyr¹⁵) and phospho-cdc25C (Ser²¹⁶) from 6 to 24 h (Figure 5A). The results from time-dependent studies indicated that decreasing functional cdc25C by increasing phosphorylation of cdc25C was followed by an increase in phospho-cdc2. Moreover, treatment with **1** also increased the expression of CDK inhibitor p21/WAF1 in HEP-2 cells (Figure 5B). These findings are consistent with reports that p21/WAF1 may help maintain G₂ cell cycle arrest by inactivating the cyclin B1/cdc2 complex in a p53-independent manner.⁴¹ Thus, it may be suggested that **1** arrests HEP-2 cells in the G₂/M phase through CDK inhibitor upregulation and the CDK-inhibition pathway. On the other hand, the present results also showed a relationship between p21/WAF1 levels and the amount of apoptosis, as **1** caused a reduction in p21/WAF1 after 24 h of treatment (Figure 5B), which was synchronous with a concomitant increase in apoptosis. An alternative postulation is that p21/WAF1 is cleaved after 12 h of oridonin treatment, and this has been proved to be a critical step in converting cells from growth arrest to undergoing apoptosis.⁴²

Recently, evidence has accumulated that ROS may also play an important role in cell-cycle progression.⁴³ In response to oxidative stress, the protein Cdc25c is phosphorylated, and this prevents the activation of Cdc2/cyclin B1 complex, thereby leading to the arrest of the G₂/M transition.⁴⁴ In the present study, addition of NAC and CAT to oridonin-treated HEP-2 cells markedly inhibited the

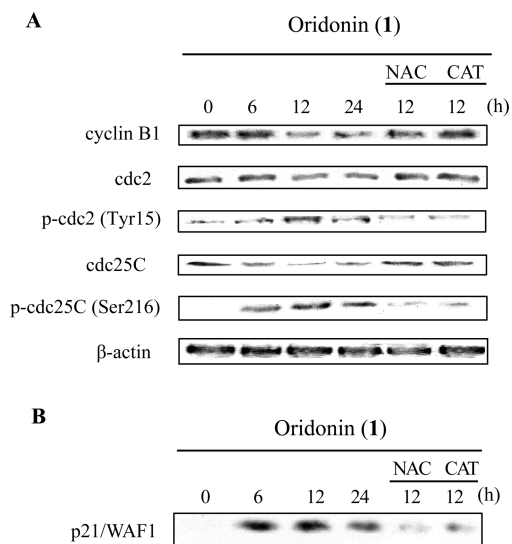


Figure 5. Oridonin (**1**) induced the changes in cell-cycle regulatory protein expression to undergo G₂/M arrest in HEP-2 cells, and ROS might play an important role in cell-cycle progression. The cells were treated with 36 μ M **1** for the indicated time periods in the absence or presence of 2.5 mM NAC or 500 U/mL CAT; then cell lysates were separated by 12% SDS-PAGE, and cyclin B1, cdc2, p-cdc2, cdc25C, and p-cdc25C (A) and p21/WAF1 (B) protein expression was detected by western blot analysis. The results shown here are representative of at least three independent experiments.

alterations in the cell cycle regulatory proteins, including cdc25C, phosphor-cdc25C, phosphor-cdc2, cdc2, and cyclin B1 as well as p21/WAF1 protein (Figure 5), suggesting that the expression of G₂/M-related cell cycle regulatory proteins might be directly affected by ROS generation, and ROS was indeed responsible for the **1**-induced cell cycle arrest. As suggested earlier,⁴⁵ induction of p21 under the conditions of oxidative stress acts through a p53-independent pathway. The present findings also suggest that **1** promoted ROS participating in the G₂/M phase arrest in a p53-independent manner in HEP-2 cells.

An important characteristic of HEP-2 cells is that they have a mutated, inactive p53 gene.^{21,22} Cells with such a mutated p53 gene tend to be resistant to the induction of apoptosis.^{15,16} However, the present study has shown that HEP-2 human laryngeal cancer cells are sensitive to growth inhibition by oridonin (**1**). The reduced survival of HEP-2 cells after exposure to **1** is associated with G₂/M phase cell cycle arrest and apoptosis induction. Oridonin-induced cell growth inhibition in the HEP-2 cells is mediated by the production of ROS, which may help to induce cell apoptosis through the mitochondrial signaling pathway and a caspase-9-independent apoptotic mechanism. In addition, ROS also contribute to **1**-induced G₂/M phase arrest through upregulation of the CDK inhibitor and CDK-inhibition pathway. Together, these findings characterize a basic mechanism through which **1** potentially could be effective in antineoplastic therapy for laryngeal cancer.

Experimental Section

Chemicals and Reagents. Oridonin (**1**) was isolated from *Rabdosia rubescens* and was identified by comparing its physical and spectroscopic (¹H NMR, ¹³C NMR) data with those reported in the literature.⁴⁶ The purity was measured by HPLC [column: 4.6 mm \times 150 mm, Inertsil ODS-SP, 5 μ m; solvent phase: methanol/H₂O, 55:45] and determined to be 99.6%. Compound **1** was dissolved in dimethyl sulfoxide (DMSO) to obtain a stock solution. The DMSO concentration was kept below 0.05% in all cell cultures used and did not exert any detectable effect on cell growth or cell death. Fetal bovine serum (FBS) was obtained from TBD Biotechnology Development (Tianjin, People's Republic of China); RPMI 1640 medium was obtained from Gibco/BRL (Gaithersburg, MD). 3-(4,5-Dimethylthiazol-2-yl)-2,5-diphenyltetrazo-

razolium bromide (MTT), 3,3-diaminobenzidine tetrahydrochloride (DAB), NAC, CAT, AO, PI, rhodamine-123, and DCF-DA were purchased from Sigma (St. Louis, MO). z-VAD-fmk, z-DEVD-fmk, Ac-LEHD-cmk, and antibodies against caspase-9 and -3 were obtained from Calbiochem (La Jolla, CA). Polyclonal antibodies against Bax, Bcl-2, cytochrome *c*, AIF, ICAD, cdc2, phospho-cdc2, cdc25c, phospho-cdc25c, cyclin B1, p21/WAF1, β -actin, and horseradish peroxidase (HRP)-conjugated secondary antibodies were obtained from Santa Cruz (Santa Cruz, CA).

Cell Culture. HEP-2 human laryngeal cancer cells were obtained from the American Type Culture Collection (ATCC, Manassas, VA). The cells were cultured in RPMI-1640 medium supplemented with 10% FBS, 10 μ g/mL streptomycin, 100 U/mL penicillin, and 0.03% L-glutamine and maintained at 37 °C with 5% CO₂ in a humidified atmosphere.

Cytotoxicity Assays. HEP-2 cells were incubated in 96-well tissue culture plates (NUNC, Roskilde, Denmark) at a density of 1.2×10^4 cells/well. After 24 h incubation, the cells were treated with or without Ac-LEHD-cmk, z-VAD-fmk, or z-DEVD-fmk at the given concentrations for 1 h and subsequently treated with oridonin (**1**) for different time periods. The cytotoxic effect was measured using the MTT assay, as described elsewhere.⁶

Flow Cytometric Analysis of Apoptosis and Cell Cycle Arrest. After chemical treatment, 1×10^6 cells were harvested, washed with PBS, then fixed with 70% ethanol, and, finally, maintained at 4 °C for at least 12 h. Then, the cell pellets were stained with the fluorescent probe solution containing 50 μ g/mL PI and 1 mg/mL DNase-free RNaseA in PBS on ice in the dark for 30 min. DNA fluorescence of PI-stained cells was evaluated by FACSscan flow cytometry (Becton Dickinson, Franklin Lakes, NJ). A minimum of 10 000 cells were analyzed per sample, and the DNA histograms were gated and analyzed further using Modfit software on a Mac workstation to estimate the percentage of cells in various phases of the cell cycle.⁸

Measurement of Intracellular ROS Generation. After treatment with 36 μ M oridonin (**1**) for the indicated time periods, the cells were incubated with 10 mM DCF-DA at 37 °C for 15 min. The intracellular ROS mediated oxidation of DCF-DA to the fluorescent compound 2',7'-dichlorofluorescein (DCF). Then, the cells were harvested and the pellets were suspended in 1 mL of PBS. Samples were analyzed at an excitation wavelength of 480 nm and an emission wavelength of 525 nm by FACSscan flow cytometry.⁴⁷

Determination of Mitochondrial Membrane Potential. Mitochondrial membrane potential was measured using the fluorescent dye rhodamine-123, as described elsewhere.⁴⁸ After incubation with 36 μ M oridonin (**1**) for the indicated time periods, the cells were stained with 1 μ g/mL rhodamine-123 and incubated at 37 °C for 15 min. The fluorescence intensity of cells in situ was observed using fluorescence microscopy. Quantitative assays were performed by a similar staining procedure to that described above. After treatment with **1**, the cells were collected and suspended in 1 mL of PBS containing 1 μ g/mL rhodamine-123 and incubated at 37 °C for 15 min. The fluorescence intensity of the cells was analyzed by FACSscan flow cytometry.

Western Blot Analysis. HEP-2 cells were cultured for different time periods, and then western blot analysis was carried out. Briefly, the cell pellets were resuspended in lysis buffer consisting of 50 mM Hepes (pH 7.4), 1% Triton-X 100, 2 mM sodium orthovanadate, 100 mM sodium fluoride, 1 mM edetic acid, 1 mM PMSF, 10 mg/L aprotinin, and 10 mg/L leupeptin and lysed at 4 °C for 60 min. After centrifugation at 13000g for 15 min, the protein content of the supernatant was determined by a protein assay reagent (Bio-Rad, Hercules, CA). The protein lysates were separated by electrophoresis on 12% SDS-polyacrylamide gel and transferred to a nitrocellulose membrane (Amersham Biosciences, Piscataway, NJ). The membranes were soaked in blocking buffer (5% skimmed milk). Proteins were detected using polyclonal antibodies and visualized using anti-rabbit or anti-mouse IgG conjugated with HRP and DAB as the HRP substrate.

Statistical Analysis of the Data. All the presented data and results were confirmed in at least three independent experiments. The data are expressed as means \pm SD. Statistical comparisons were made by Student's *t*-test, and *p* < 0.05 was considered statistically significant.

Acknowledgment. The authors would like to acknowledge Ms. Y. Mu for technical assistance.

Supporting Information Available: Cytotoxicity of oridonin (**1**) against HEP-2 cells, observation of apoptotic cell morphological changes, FACS images of **1**-induced ROS generation, and fluorescent and FACS images of **1**-induced $\Delta\Psi_m$ changes. This material is available free of charge via the Internet at <http://pubs.acs.org>.

References and Notes

- Newman, D. J.; Cragg, G. M. *J. Nat. Prod.* **2007**, *70*, 461–477.
- Fujita, T.; Takeda, Y.; Sun, H. D.; Minami, Y.; Marunaka, T.; Takeda, S.; Yamada, Y.; Togo, T. *Planta Med.* **1988**, *54*, 414–417.
- Osawa, K.; Yasuda, H.; Maruyama, T.; Morita, H.; Takeya, K.; Itokawa, H. *Phytochemistry* **1994**, *36*, 1287–1291.
- Lee, J. H.; Koo, T. H.; Hwang, B. Y.; Lee, J. J. *J. Biol. Chem.* **2002**, *277*, 18411–18420.
- Zhang, H.; Fan, Z.; Tan, G. T.; Chai, H.-B.; Pezzuto, J. M.; Sun, H.-D.; Fong, H. H. S. *J. Nat. Prod.* **2002**, *65*, 215–217.
- Huang, J.; Wu, L. J.; Tashiro, S.; Onodera, S.; Ikejima, T. *J. Pharmacol. Sci.* **2008**, *107*, 370–379.
- Zhou, G. B.; Kang, H.; Wang, L.; Gao, L.; Liu, P.; Xie, J.; Zhang, F. X.; Weng, X. Q.; Shen, Z. X.; Chen, J.; Gu, L. J.; Yan, M.; Zhang, D. E.; Chen, S. J.; Wang, Z. Y.; Chen, Z. *Blood* **2007**, *109*, 3441–3445.
- Zhang, Y.; Wu, Y.; Wu, D.; Tashiro, S.; Onodera, S.; Ikejima, T. *Arch. Biochem. Biophys.* **2009**, *489*, 25–33.
- Marioni, G.; Marchese-Ragona, R.; Cartei, G.; Marchese, F.; Staffieri, A. *Cancer Treat. Rev.* **2006**, *32*, 504–515.
- Rafferty, M. A.; Fenton, J. E.; Jones, A. S. *Clin. Otolaryngol. Allied Sci.* **2001**, *26*, 442–446.
- Fei, S. Z. *Epidemic Feature of Larynx Carcinoma, Oncology of Head and Neck*; Tianjin Science and Technology: Tianjin, China, 1993; pp 659–660.
- Chaigneau, L.; Guardiola, E.; N'Guyen, T.; Dufresne, A.; Stein, U.; Villanueva, C.; Thiery-Vuillemin, A.; Lorchel, F.; Pivot, X. *Bull. Cancer* **2006**, *93*, 677–682.
- Taguchi, T.; Tsukuda, M. *Gan To Kagaku Ryoho* **2005**, *32*, 2030–2034.
- Vousden, K. H. *Cell* **2000**, *103*, 691–694.
- Giaccia, A. J.; Kastan, M. B. *Genes Dev.* **1998**, *12*, 2973–2983.
- Kinzel, K. W.; Vogelstein, B. *Nature* **1996**, *379*, 19–20.
- Farhadieh, R. D.; Smece, R.; Rees, C. G.; Salardini, A.; Eggleton, S.; Yang, J. L.; Russell, P. J. *Aust. NZ. J. Surg.* **2009**, *79*, 48–54.
- Zhao, X.; Li, F. C.; Li, Y. H.; Fu, W. N.; Huang, D. F.; Ye, Y.; Xu, Z. M.; Sun, K. L. *Zhonghua Zhong Liu Za Zhi* **2005**, *27*, 134–137.
- Hostanska, K.; Vuong, V.; Rocha, S.; Soengas, M. S.; Glanzmann, C.; Saller, R.; Bodis, S.; Pruschy, M. *Br. J. Cancer* **2003**, *88*, 1785–1792.
- Khan, M.; Giessrigl, B.; Vonach, C.; Madlener, S.; Prinz, S.; Herbacek, I.; Hölzl, C.; Bauer, S.; Viola, K.; Mikulits, W.; Quereshi, R. A.; Knasmüller, S.; Grusch, M.; Kopp, B.; Krupitza, G. *Mutat. Res.* **2010**, *683*, 123–130.
- Kraljevic-Pavelic, S.; Cacev, T.; Kralj, M. *Cancer Gene Ther.* **2008**, *15*, 576–901.
- Taron, M.; Plasencia, C.; Abad, A.; Martin, C.; Guillot, M. *Invest. New Drugs* **2000**, *18*, 139–147.
- Bunz, F.; Dutriaux, A.; Lengauer, C.; Waldman, T.; Zhou, S.; Brown, J. P.; Sedivy, J. M.; Kinzler, K. W.; Vogelstein, B. *Science* **1998**, *282*, 1497–1501.
- Molinari, M. *Cell Prolif.* **2000**, *33*, 261–274.
- Moungjaroen, J.; Nimmannit, U.; Callery, P. S.; Wang, L.; Azad, N.; Lipipun, V.; Chanvorachote, P.; Rojanasakul, Y. *J. Pharmacol. Exp. Ther.* **2006**, *319*, 1062–1069.
- Pelicano, H.; Carney, D.; Huang, P. *Drug Resist. Updates* **2004**, *7*, 97–110.
- Narvaez, C. J.; Welsh, J. J. *Biol. Chem.* **2001**, *276*, 9101–9107.
- Chen, C. Y.; Chen, C. H.; Lo, Y. C.; Wu, B. N.; Wang, H. M.; Lo, W. L.; Yen, C. M.; Lin, R. J. *J. Nat. Prod.* **2008**, *71*, 933–940.
- Hong, C.; Firestone, G. L.; Boeldanes, L. F. *Biochem. Pharmacol.* **2002**, *63*, 1085–1097.
- Tsujimoto, Y. *Genes Cells* **1998**, *3*, 697–707.
- Green, D. R.; Reed, J. C. *Science* **1998**, *281*, 1309–1312.
- van Gurp, M.; Festjens, N.; van Loo, G.; Saelens, X.; Vandennebeele, P. *Biochem. Biophys. Res. Commun.* **2003**, *304*, 487–497.
- Daugas, E.; Nochy, D.; Ravagnan, L.; Loeffler, M.; Susin, S. A.; Zamzami, N.; Kroemer, G. *FEBS Lett.* **2000**, *476*, 118–123.
- Salvesen, G. S.; Dixit, V. M. *Cell* **1997**, *91*, 443–446.
- Zhang, C. L.; Wu, L. J.; Tashiro, S.; Onodera, S.; Ikejima, T. *J. Asian Nat. Prod. Res.* **2004**, *6*, 127–138.
- Sakahira, H.; Enari, M.; Nagata, S. *J. Biol. Chem.* **1999**, *274*, 15740–15744.
- Danial, N. N.; Korsmeyer, S. *Cell* **2004**, *116*, 205–219.
- Kaufmann, S. H.; Hengartner, M. O. *Trends Cell Biol.* **2001**, *11*, 526–534.

- (39) Zheng, T. S.; Hunot, S.; Kuida, K.; Momoi, T.; Srinivasan, A.; Nicholson, D. W.; Lazebnik, Y.; Flavell, R. A. *Nat. Med.* **2000**, *6*, 1241–1247.
- (40) Lee, S. M.; Kwon, J. I.; Choi, Y. H.; Eom, H. S.; Chi, G. Y. *Phytother. Res.* **2008**, *22*, 752–758.
- (41) Choi, Y. H.; Lee, W. H.; Park, K. Y.; Zhang, L. J. *Cancer Res.* **2000**, *91*, 164–173.
- (42) Zhang, Y.; Fujita, N.; Tsuruo, T. *Oncogene* **1999**, *18*, 1131–1138.
- (43) Boonstra, J.; Post, J. A. *Gene* **2004**, *337*, 1–13.
- (44) Sanchez, Y.; Wong, C.; Thoma, R. S.; Richman, R.; Wu, Z.; Pivnicka-Worms, H.; Elledge, S. J. *Science* **1997**, *277*, 1497–1501.
- (45) Russo, T.; Zamrano, N.; Esposito, F.; Ammendola, R.; Cimino, F.; Fiscella, M.; Jackman, J.; O'Connor, P. M.; Anderson, C. W.; Apella, F. *J. Biol. Chem.* **1995**, *270*, 29386–29391.
- (46) Lu, Y. B.; Sun, C. R.; Pan, Y. J. *J. Sep. Sci.* **2006**, *29*, 314–318.
- (47) Yang, M. L.; Huang, T. S.; Lee, Y.; Lu, F. J. *Free Radical Res.* **2002**, *36*, 685–693.
- (48) Saris, N. E.; Teplova, V. V.; Odinkova, I. V.; Azarashvily, T. S. *Anal. Biochem.* **2004**, *328*, 109–112.

NP9008199